ACS APPLIED MATERIALS & INTERFACES

Research Article

www.acsami.org

# Förster Resonance Energy Transfer Studies of Luminescent Gold Nanoparticles Functionalized with Ruthenium(II) and Rhenium(I) Complexes: Modulation via Esterase Hydrolysis

Frankie Chi-Ming Leung, Anthony Yiu-Yan Tam, Vonika Ka-Man Au, Mei-Jin Li, and Vivian Wing-Wah Yam*

Institute of Molecular Functional Materials (Areas of Excellence Scheme, University Grants Committee (Hong Kong)) and Department of Chemistry, The University of Hong Kong, Pokfulam Road, Hong Kong SAR, P. R. China

Supporting Information

**ABSTRACT:** A number of ruthenium(II) and rhenium(I) bipyridine complexes functionalized with lipoic acid moieties have been synthesized and characterized. Functionalization of gold nanoparticles with these chromophoric ruthenium(II) and rhenium(I) complexes has resulted in interesting supramolecular assemblies with Förster resonance energy transfer (FRET) properties that could be modulated via esterase hydrolysis. The luminescence of the metal complex chromophores was turned on upon cleavage of the ester bond linkage by esterase to reduce the efficiency of FRET quenching. The prepared nanoassembly conjugates have been characterized by transmission electron microscopy (TEM), energy-dispersive X-ray analysis (EDX), Fourier transform infrared spectroscopy (FTIR), dynamic light scattering (DLS), UV−visible spectroscopy, and emission spectroscopy. The quenching mechanism has also been studied by transient absorption and time-resolved emission decay measurements. The FRET efficiencies were found to vary with the nature of the chromophores and the length of the spacer between the donor (transition metal complexes) and the acceptor (gold nanoparticles).

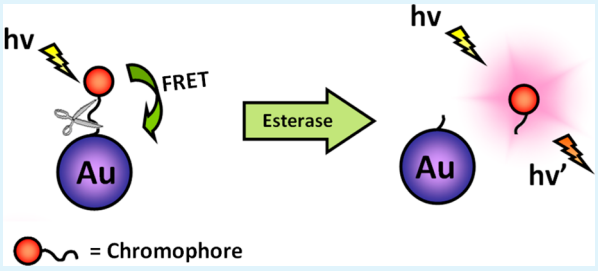


**KEYWORDS:** *gold nanoparticles, ruthenium(II), rhenium(I), FRET, esterase, transient absorption*

## INTRODUCTION

Over the past two decades, there has been a significant interest in the study of Förster resonance energy transfer (FRET), which has been proved to be an important strategy for the applications in molecular and supramolecular photophysics,[1−4] biology,[5−10] and molecular devices.[11−18] Such an energy transfer mechanism can provide more valuable information on the response of the interactions between the donor and the acceptor under external perturbations. Because this process is strongly distance- and orientation-dependent, the efficiency and the rate of energy transfer can be modified mutually by variation of the spacer distance or simply by cleavage of the linker. In recent years, some ratiometric fluorescent sensors based on FRET have been developed for protease sensing.[6,19,20] Recently, we demonstrated that the determination of the enzymatic activity of esterase can be realized via a simple bimolecular system based on the intramolecular energy transfer mechanism for the recovery of the $^3$MLCT emission of ruthenium(II) complexes and the system has been applied for the imaging of living HepG2 cells.[21]

On the other hand, there has been an increasing interest in the research in applying nanotechnology for creating chemical and biological sensors due to the unique photophysical properties and quantum size effect of nanoparticles that are absent in the macroscopic world.[22,23] In particular, gold nanoparticles (GNPs) have well been known as superb emission quenchers due to their broad surface plasmon resonance (SPR) absorption in the UV−visible (UV−vis) region, and spherical GNPs have been found to quench the excited state energy of the donor from all orientations.[24,25] Apart from these, other advantages of the use of GNPs as a platform for the design of the system include the ready tuning of their optical and plasmonic properties by a variation in their size, shape, and the surrounding environment, their ready and facile synthesis to give GNPs of high stability, and their ability to overcome the limitations of FRET for traditional organic quenchers.[26] The detection length scale of molecular donor−acceptor systems based on FRET is limited by the dipole−dipole moment, which constrains the Förster radius $R_0$ to the order of <100 Å. According to the literature,[26] the surface plasmon resonances can enhance the energy transfer rate by an order of $10^4$−$10^5$. The calculated energy transfer distances can achieve the range of 70−100 nm, which is ∼10 times longer than the typical Förster distances ($R_0$). The incorporation of organic dyes with GNPs has been widely exploited as biological probes.[27−33] However, the luminescence lifetime of organic

Received: January 17, 2014
Accepted: April 8, 2014
Published: April 22, 2014

  

**Scheme 1. Chemical Structures of Complexes 1−5**

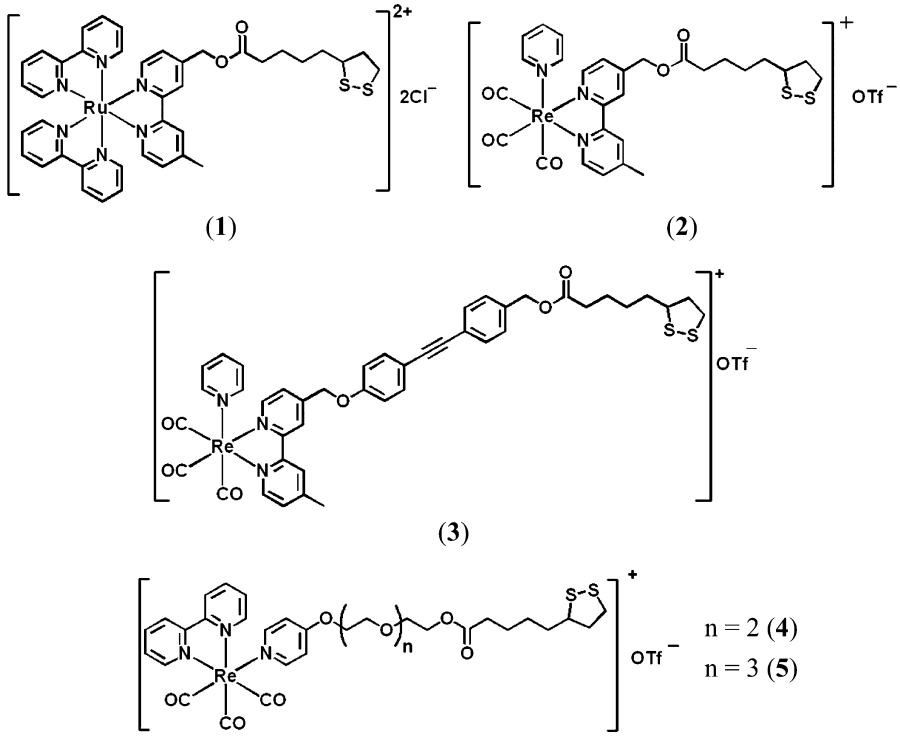


**Scheme 2. Cartoon Representation of the Corresponding GNP Systems of the Complexes**

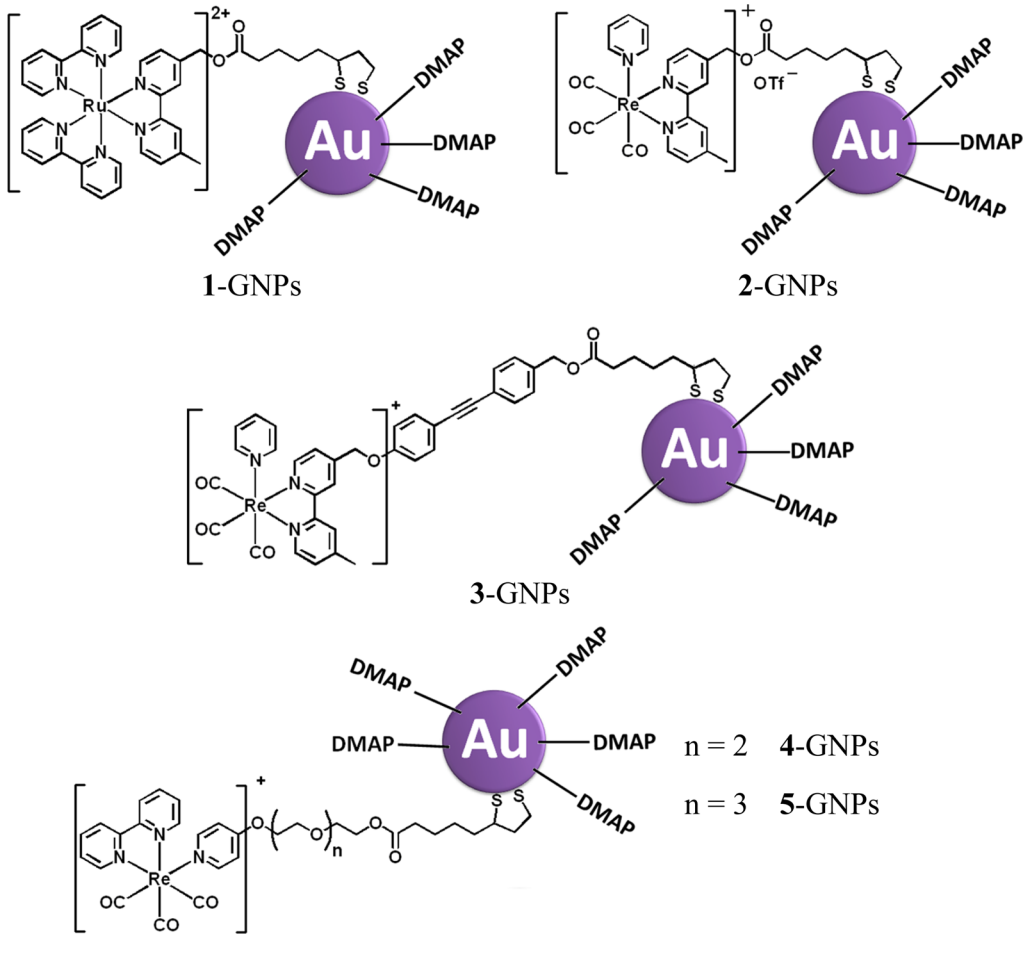



dx.doi.org/10.1021/am500350c | ACS Appl. Mater. Interfaces 2014, 6, 6644−6653

**Table 1. Photophysical Data of Complexes 1−5**

| | absorption[a] | emission | | |
|---|---|---|---|---|
| complex | $\lambda_{abs}$/nm ($\varepsilon$/dm$^3$ mol$^{-1}$ cm$^{-1}$) | medium ($T$/K) | $\lambda_{em}$/nm ($\tau_0$/$\mu$s) | $\Phi_{lum}$[c] |
| **1** | 246 (26445), 256 (23030), 288 sh (64840), 326 (11050), 426 (11315), 456 (13920) | buffer (298)[a] | 625 (0.56) | 0.05 |
| | | glass (77)[b] | 585 (4.73), 635 (4.70) | |
| **2** | 251 (18400), 304 (11700), 318 (10800), 346 (4250) | buffer (298)[a] | 563 (0.21), 606 (0.21) | 0.011 |
| | | glass (77)[b] | 507 (5.32), 546 (5.31) | |
| **3** | 255 (20335), 291 (29550), 309 (25565), 349 (3465) | buffer (298)[a] | 564 (0.19), 610 (0.19) | 0.010 |
| | | glass (77)[b] | 508 (5.31), 547 (5.30) | |
| **4** | 251 (22255), 306 (10800), 320 (11225), 356 (3745) | buffer (298)[a] | 564 (0.16), 609 (0.16) | 0.021 |
| | | glass (77)[b] | 510 (5.20), 546 (5.19) | |
| **5** | 250 (23775), 306, (11060)320 (11720), 357 (3700) | buffer (298)[a] | 564 (0.15), 607 (0.15) | 0.018 |
| | | glass (77)[b] | 509 (5.18), 547 (5.17) | |

[a]In degassed Tris-HCl (10 mM, pH 8.0)−MeOH (95:5 v/v) at 298 K. [b]In EtOH−MeOH (4:1 v/v). [c]The luminescence quantum yield, measured at room temperature using $[Ru(bpy)_3]Cl_2$ (for **1**) and quinine sulfate (for **2**−**5**) as a standard

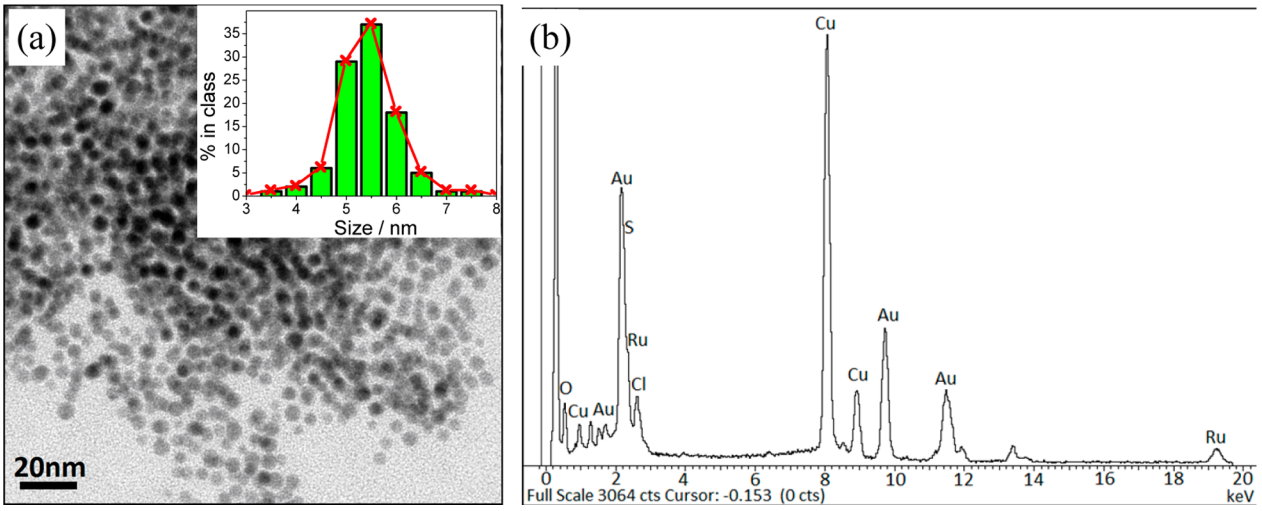


**Figure 1.** (a) TEM image of **1**-GNPs. Inset: particle size distribution. (b) EDX spectrum of **1**-GNPs.

dyes is relatively short when compared to that of the transition metal complexes. Owing to the advantages of the long-lived luminescence behavior of the triplet state, the large Stokes shift, and the ready tunability of the emission energies, transition metal complexes can provide a better control of the spectral overlap between the emission band of the transition metal complexes moiety and the SPR band of GNPs, which can enhance the energy transfer efficiency between them.[34,35] However, the coordination of metal complexes onto GNPs is still relatively less explored and the quenching mechanism between them are relatively poorly understood.[36−40] Inorganic−organic hybrid systems of GNPs functionalized with transition metal systems are also relatively less explored. As an extension of our previous work, herein we report the preparation of water-soluble luminescent ruthenium(II) and rhenium(I) polypyridine complexes (Scheme 1) and their functionalized GNPs (Scheme 2) and a "proof-of-principle" concept for the detection of esterase through a modulation of the FRET properties. Transient absorption spectroscopy and time-resolved emission studies have been performed to provide insights into the quenching mechanism. The length of the linker between the luminophores and the GNPs has been varied to study its effect on the quenching efficiency.

## RESULTS AND DISCUSSION

**Synthesis, Characterization, and Photophysical Study of Complexes.** Ruthenium(II) complex **1** and rhenium(I) complexes **2**−**5** were synthesized according to the literature reported procedures with slight modifications.[18,41,42] The identities of all the ligands and complexes were confirmed by satisfactory $^1$H NMR spectroscopy, EI or ESI mass spectroscopy, infrared spectroscopy, and elemental analyses (see Supporting Information for characterization data and experimental procedures).

The photophysical data of complexes **1**−**5** were tabulated in Table 1. The electronic absorption spectrum of ruthenium(II) complex **1** in buffer solution (Tris-HCl (10 mM, pH 8.0)−MeOH (95:5 v/v)) showed an intense band at ca. 288 nm, ascribed to the intraligand (IL) $\pi \rightarrow \pi^*$ transition of bipyridine. The less intense bands at ca. 450 nm are assigned as the spin-allowed metal-to-ligand charge transfer MLCT[d$\pi$(Ru) → $\pi^*$(bpy)] transitions, typical of ruthenium(II) tris-bipyridine complex systems.[43−47] The electronic absorption spectra of the rhenium(I) complexes, complexes **2**−**5** in buffer solution showed intense high-energy absorption bands with molar extinction coefficients in the order of $10^4$ dm$^3$ mol$^{-1}$cm$^{-1}$ at ca. 300 nm, which are assigned as intraligand (IL) $\pi \rightarrow \pi^*$ transitions of the pyridine and bipyridine moieties. The lower energy absorption bands at ca. 350 nm with molar extinction coefficients in the order of $10^3$ dm$^3$ mol$^{-1}$ cm$^{-1}$ were ascribed

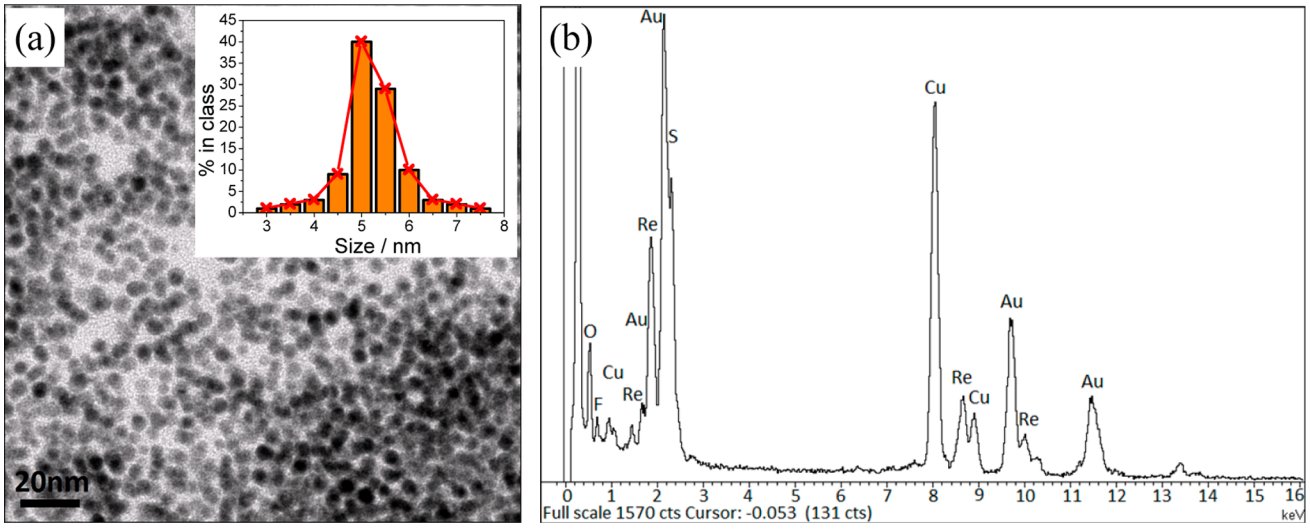


**Figure 2.** (a) TEM image of **2**-GNPs. Inset: particle size distribution. (b) EDX spectrum of **2**-GNPs.

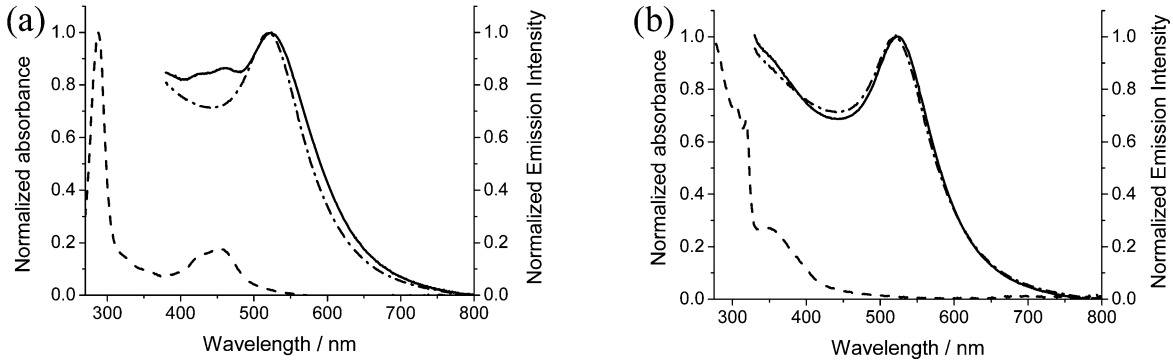


**Figure 3.** (a) Electronic absorption spectra of complex **1** (– – –), DMAP-GNPs (– - –) and **1**-GNPs (—) in water–MeOH (95:5 v/v). (b) Electronic absorption spectra complex **2** (– – –), DMAP-GNPs (– - –) and **2**-GNPs (—) in water–MeOH (95:5 v/v).

to the spin-allowed MLCT[d$\pi$(Re) → $\pi$*(bpy)] transitions, typical of rhenium(I) tricarbonyl diimine complex systems.[18,48−50]

Upon excitation of complex **1** at 456 nm in degassed buffer solution at room temperature, a low-energy emission band at ca. 625 nm was observed. The large Stokes shift together with the relatively long radiative lifetime observed were suggestive of an emissive origin of triplet parentage, derived from the $^3$MLCT[d$\pi$(Ru) → $\pi$*(bpy)] state. The emission energy of the complex was comparable to those of other ruthenium(II) tris-bipyridine complex systems.[43−47] On the other hand, excitation of complex **2** in degassed buffer solution at 346 nm at room temperature gave rise to a long-lived intense emission at ca. 563 nm. The emission band was assigned as originated from excited states of $^3$MLCT[d$\pi$(Re) → $\pi$*(bpy)] character with some mixing of intraligand $\pi$ → $\pi$* character.[17,18,48−50] The emission bands for complexes **3**−**5** were assigned similarly.

**Preparation and Characterization of GNPs.** DMAP-capped GNPs have been employed for the incorporation of the transition metal complexes. The advantages of using DMAP-capped GNPs are threefold. The first is their water solubility, which would enable studies in the biological environment. Second is the lability for exchange with thiolate molecules to occur. The third is the positive surface charge, which would prevent the aggregation of the GNPs by the electrostatic repulsion between the cationic metal complex and the positive charge of the DMAP capping agent. The functionalized GNPs were synthesized according to the literature with slight modifications.[51−56]

From the TEM image of **1**-GNPs (Figure 1a), the average particle size was 5.4 nm. On the other hand, the size of **2**-GNPs (Figure 2a) was 5.2 nm. By using dynamic light scattering (DLS), the hydrodynamic diameters of **1**-GNPs and **2**-GNPs were 21.4 and 20.4 nm, respectively. The particle size distributions of the GNPs have also been shown to give satisfactory dispersity (Supporting Information Figure S1). The energy-dispersive X-ray (EDX) of **1**-GNPs (Figure 1b) and **2**-GNPs (Figure 2b) showed the characteristic peaks of ruthenium and rhenium, respectively, similar to that of the reported EDX spectrum of other transition metal complex functionalized GNPs,[57,58] supporting the successful preparation of **1**-GNP and **2**-GNPs. FTIR studies of **1**-GNPs (Supporting Information Figure S2) showed the $\nu$(C═O) stretch, typical of the ester group of complex **1**. Similarly, for **2**-GNPs (Supporting Information Figure S3), the three characteristic stretches of the carbonyl ligands of complex **2**, together with the $\nu$(C═O) of the ester linkage, were observable, confirming the successful attachment of the complexes on the GNPs. By using the tight packed spherical model of the gold nanoclusters and thermogravimetric analysis (TGA) studies (Supporting Information Figure S4−S6),[59,60] the surface coverages of complex **1** and **2** were estimated to be 57% and 71%, respectively (see ESI for the calculations). The electronic


dx.doi.org/10.1021/am500350c | ACS Appl. Mater. Interfaces 2014, 6, 6644−6653

**Table 2. Physical Properties of the GNPs**

| | average size (nm) | hydrodynamic diameter (nm) | SPR band (nm) | luminescence quantum yield[b] | complex loading (%) | surface coverage (%) |
|---|---|---|---|---|---|---|
| DMAP-GNPs | 4.8 | 15.2 ± 4.6 | 520 | *a* | | 87 |
| **1**-GNPs | 5.4 | 21.4 ± 12.5 | 524 | 0.0056 | 30.9 | 57 |
| **2**-GNPs | 5.2 | 20.4 ± 9.5 | 523 | 0.0011 | 19.2 | 71 |

[a]Nonemissive. [b]The luminescence quantum yield, measured at room temperature using $[Ru(bpy)_3]Cl_2$ (for **1**-GNPs) and quinine sulfate (for **2**-GNPs) as a standard

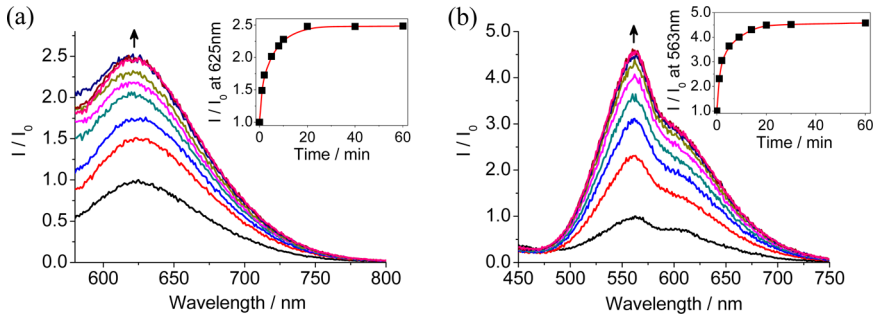


**Figure 4.** Time-dependent changes in emission spectra of (a) **1**-GNPs dispersed in Tris-HCl (10 mM, pH 8.0)−MeOH (95:5 v/v) over 1 h upon treatment with PLE at 25 °C with excitation wavelength at 456 nm. Inset: plot of relative emission intensity at 625 nm versus time of esterase treatment. (b) Time-dependent changes in emission spectra of **2**-GNPs dispersed in Tris-HCl (10 mM, pH 8.0)−MeOH (95:5 v/v) over 1 h upon treatment with PLE at 25 °C with excitation wavelength at 346 nm. Inset: plot of relative emission intensity at 563 nm versus time of esterase treatment.

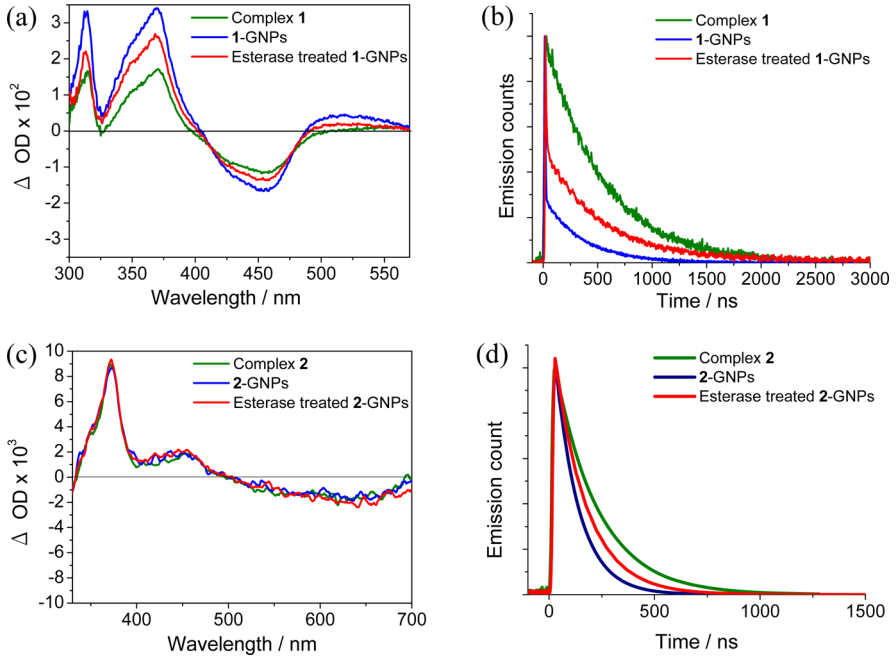


**Figure 5.** (a) Transient absorption difference spectra of free complex **1**, **1**-GNPs, and **1**-GNPs after prolonged treatment with esterase. Excitation laser was at 355 nm and emission signals were monitored at 625 nm. (b) Time-resolved emission decay of free complex **1**, **1**-GNPs, and **1**-GNPs after prolonged treatment with esterase in Tris-HCl (10 mM, pH 8.0)−MeOH (95:5 v/v). (c) Transient absorption spectra of free complex **2**, **2**-GNPs, and **2**-GNPs after prolonged treatment with esterase. Excitation laser was at 355 nm and emission signals were monitored at 560 nm. (d) Time-resolved emission decay of free complex **2**, **2**-GNPs, and **2**-GNPs after prolonged treatment with esterase in Tris-HCl (10 mM, pH 8.0)−MeOH (95:5 v/v).

absorption spectra (Figure 3) showed characteristic surface plasmon resonance (SPR) peak maximum of DMAP-GNPs at 520 nm, similar to that reported in the literature.[61] For **1**-GNPs (Figure 3a), the absorption maxima at 426 and 456 nm were found to be the spin-allowed metal-to-ligand charge transfer (MLCT) bands typical of the attached complex **1**, which were assigned as MLCT[$d\pi$(Ru) → $\pi^*$(bpy-LA)] transition and MLCT[$d\pi$(Ru) → $\pi^*$(bpy)] transition, respectively. For **2**-GNPs, the absorption maxima at 346 nm was assigned as the MLCT[$d\pi$(Re) → $\pi^*$(bpy)] transition of the attached complex **2**. The physical properties of the modified GNPs are summarized in Table 2.

**Treatment of Esterase.** The responses of the GNPs functionalized with ruthenium(II) and rhenium(I) complexes

toward porcine liver esterase have been investigated by the emission spectroscopic method. The hydrolytic cleavage of the ester linkage between the transition metal−ligand chromophores and the GNPs quencher by the enzymatic activity of esterase has been monitored by emission studies (Figure 4). Cleavage of the ester linkage was found to recover the MLCT luminescence of the chromophore. The electronic absorption spectra (Supporting Information Figure S7) of **1**-GNPs and **2**-GNPs upon treatment with porcine liver esterase (PLE) over 60 min showed that the cleavage of the ester linkage did not cause an obvious change in the electronic configuration of the complexes and GNPs. More interestingly, time-dependent studies on the emission spectral changes of **1**-GNPs (Figure 4a) at 625 nm after treatment with PLE over 1 h have been performed. The emission intensity was found to increase by about 2.5-fold over 60 min upon treatment of esterase. A similar trend could be observed for **2**-GNPs (Figure 4b), with the emission intensity increased by about 4.5-fold from the initial value. From the control experiments of the free metal complexes, cleavage of the ester bond by esterase did not lead to an increase in the emission intensity, confirming that the increase in emission intensity observed in **1**-GNPs and **2**-GNPs was solely a consequence of the release of the GNP quencher upon treatment with esterase. The slightly more efficient quenching observed in **2**-GNPs than that in **1**-GNPs might probably be attributed to a more efficient spectral overlap between the emission of Re(I) complex **2** and the SPR absorption band of GNPs than that of complex **1**.[62,63] Nonenzymatic base-catalyzed hydrolysis has not been attempted because the GNPs will suffer from aggregation problems due to the destabilization by strong bases. The Michaelis−Menten constant ($K_M$) and maximum reaction rate ($V_{max}$) of 1.78 $\mu$M and 0.917 $\mu$M min$^{-1}$, respectively, have been determined with **1**-GNPs system, while a $K_M$ and $V_{max}$ of 1.17 $\mu$M and 1.39 $\mu$M min$^{-1}$ were obtained for **2**-GNPs system (see Figure S8 in the Supporting Information for Michaelis−Menten plots).

**Transient Absorption Studies.** Several possible mechanisms have been suggested for the emission quenching by GNPs, with the most extensively reported ones being a quenching mechanism dominated by energy transfer from the chromophore to the GNPs and another by electron transfer from the attached chromophore to another adjacent molecules.[64] To study the quenching mechanism brought about by the GNPs in detail, nanosecond transient absorption (TA) measurements have been performed on complexes **1** and **2** and their corresponding modified nanoparticles before and after prolonged treatment with esterase in degassed Tris-HCl (10 mM, pH 8.0)−MeOH (95:5 v/v) solution.

The transient absorption difference spectrum of complex **1** featured two absorption peaks at around 395 nm and bleaching at around 450 nm (Figure 5a). The higher-energy band has been assigned to the triplet absorption of $[Ru^{III}(bpy)_2(bpy\text{-}LA^{-\bullet})]^{2+*}$, in accordance with the assignment for related ruthenium(II) polypyridine complexes reported in the literature.[64] The TA bands showed a monoexponential decay lifetime of ca. 535 ns. The TA spectrum of **1**-GNPs showed a new band formed at ca. 520 nm and an increase in the absorption at 308 nm, similar to that of ruthenium(II) attached GNPs reported by Kamat and co-workers.[64] According to the literature,[65] the formation of the new band was ascribed to the charge transfer product of the one-electron reduced form of ruthenium(II) complexes, which was suggestive of a charge transfer process from the adjacent unprotonated DMAP molecules to the excited ruthenium(II) complex in **1**-GNPs. Upon treatment with esterase, the band at ca. 520 nm was found to drop in intensity to close to that of free complex **1**, suggesting that after treatment with esterase, the ruthenium(II) complex would detach from the gold surface. The transient absorption decay was found to be similar to that of the emission decay time constant. From the time-resolved emission decay studies (Figure 5b), the long-lived $^3$MLCT emission of Ru(II) complex **1** has been found to change from a monoexponential decay with $\tau_1$ = 535 ns to a biexponential decay with $\tau_1$ = 359 ns (72.3%) and a short-lived $\tau_2$ = 7.81 ns (27.7%) after attaching onto the GNPs. The formation of the short-lived emission component was similar to that reported in the literature,[64] probably due to the occurrence of electron transfer quenching of excited complex **1** by the adjacent DMAP molecules. However, unlike previous related studies, the longer-lived component of the $^3$MLCT emission decay was shortened from 535 to 359 ns. A dynamic energy transfer quenching mechanism might have been involved to shorten the lifetime of the Ru(II) complex in this case. The shortened luminescence lifetime is probably due to the short distance between the chromophores and gold nanoparticles surface. Therefore, the quenching mechanism of the ruthenium(II) $^3$MLCT emission by the gold nanoparticles has been ascribed by a combination of charge transfer and dynamic energy transfer quenching. There were several possible reasons for the observed mechanism to be different from that previously studied.[64] First, the distance between the chromophores and the surface of the GNPs was relatively short when compared to the literature systems,[64] thus FRET may become more favorable. Second, energy transfer mechanisms would be more favorable for large GNPs (diameter >5 nm).[66] A large fraction of the prepared GNPs in the current study was found to have rather large diameters as seen from their size distribution (Figure 1a) for participation in the energy transfer process. Third, the surface coverage of the complex on the GNPs could also determine the efficiency of the electron transfer process because the DMAP molecules would play an important role for the quenching process. According to a report by the group of Murray,[67] the photoinduced electron transfer (PET) would only occur in GNPs with diameter less than 3 nm, which supported the lack of electron transfer to the GNPs in the present study (>5 nm). The quenching mechanism has been further supported by spacer length dependence study (vide infra). After the treatment with esterase, the luminescence decay has been found to revert back to $\tau_1$ = 505 ns (80.0%) and a short-lived component $\tau_2$ = 8.02 ns (20.0%). The decrease in the contribution of the short-lived component $\tau_2$ and increase in the contribution of the long-lived component $\tau_1$ suggested that after the cleavage of the ester bond, the electron transfer quenching by the adjacent DMAP molecules would no longer exist and the energy transfer efficiency would also be decreased as a result of the breaking of the linkage. The luminescence lifetime of the hydrolyzed form of complex **1**, $[Ru^{II}(bpy)_2(Me\text{-}bpyCH_2OH)]^{2+}$, could not be completely recovered to that of the free unhydrolyzed complex **1**. The reason may probably be due to the different excited state lifetimes of the unhydrolyzed and hydrolyzed forms of complex **1** as they are essentially two different complexes, which cannot have identical excited state properties, lifetimes, and photoluminescence quantum yields. It might also be due to the presence of other intermolecular quenching pathways between the free hydrolyzed complex and

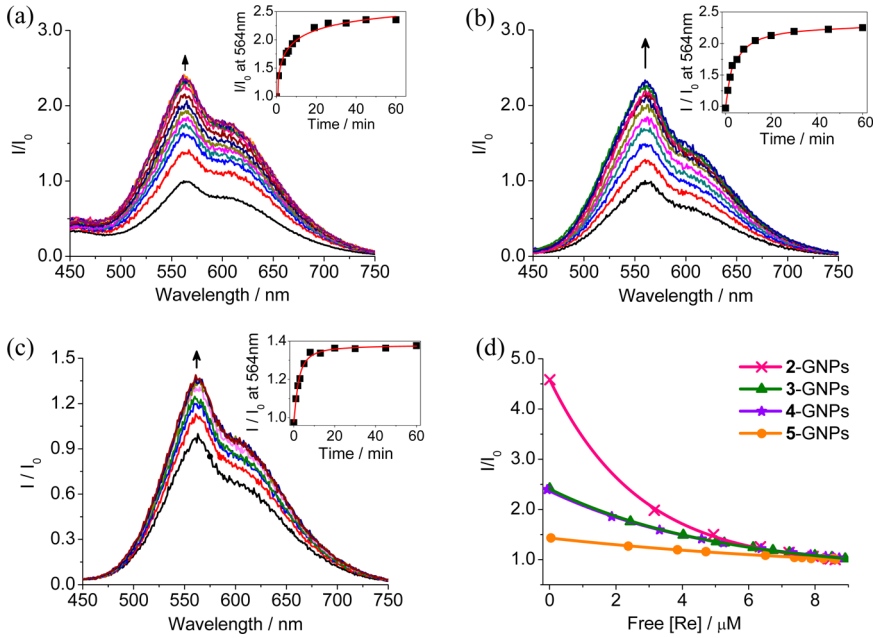


**Figure 6.** Time-dependent changes in emission spectra of (a) **3**-GNPs, (b) **4**-GNPs, and (c) **5**-GNPs dispersed in Tris-HCl (10 mM, pH 8.0)−MeOH (95:5 v/v) over 1 h upon treatment with PLE at 25 °C with excitation wavelength at 346 nm. Inset: plot of relative emission intensity at 564 nm versus time of esterase treatment. (d) The Stern−Volmer plot (concentration of Re(I) complexes hydrolyzed against $I/I_0$) of different rhenium(I) complexes.

the gold colloids. Interestingly, the drop of the luminescence intensity of complex **1** upon attachment to the GNPs was found to be greater than the corresponding drop in the excited state lifetime, suggesting that the quenching process did not only involve dynamic FRET quenching as revealed by excited state lifetime measurements but also static quenching in the presence of the GNPs. The occurrence of the SPR band of GNPs at similar wavelength region as the complex emission may also give rise to self-absorption or reabsorption phenomenon that reduces the luminescence intensity.

The TA spectrum of Re(I) complex **2** was characterized by absorption maxima at 345, 390, and 470 nm (Figure 5c). The spectrum was typical of tricarbonyl Re(I) polypyridine complexes of the related $[Re(CO)_3(bpy)(py)]^+$.[68,69] The TA bands showed a similar monoexponential decay lifetime of 207 ns. Upon attachment of complex **2** onto the GNPs, the transient absorption did not show a significant change, with no electron transfer products being generated. Different from the case of Ru(II), the presence of a shorter-lived species was not obvious. As the luminescence lifetime of complex **2** was found to be significantly shorter than that of complex **1**, it was believed that the short-lived component could not be readily resolved from the excited state of the GNP-free complex due to the closeness of their excited state lifetimes and the limitation exerted by the laser pulse width (8−10 ns) of the instrument. From the time-resolved emission decay studies (Figure 5d), the monoexponential $^3$MLCT emission lifetime of **2** was found to drop significantly from 207 to 112 ns after the attachment of **2** onto the GNPs. Such an observation was typical of energy transfer quenching of the triplet excited state by GNPs,[70] suggesting that a dynamic energy transfer quenching mechanism has occurred. Interestingly, after the treatment with esterase, the decay lifetime was raised back to 151 ns.

**Effect of the Length of the Spacer.** To further confirm the energy transfer quenching mechanism of the GNPs, complexes **3**, **4**, and **5** have been synthesized and attached onto the GNPs to study the effect of the length of the spacer. Complex **3** contains a rigid linker with broken conjugation by a $-CH_2$ group in the middle portion of the linker so that the conjugation would not affect the energy of the emission. The polyphenylene linker is sufficiently rigid to prevent the close contact between the chromophore and the GNPs. Figure 6a shows the time-dependent changes in the emission spectra of **3**-GNPs upon treatment with esterase in buffer solution. The emission intensity was found to increase by 2.5-fold in 60 min. When compared to **2**-GNPs, the increase in emission intensity for **3**-GNPs occurred to a smaller extent. The much smaller change was probably due to the poorer efficiency of energy transfer upon an increase in the spacer length.

For complexes **4** and **5**, there are long oligoether chains to separate the Re(I) chromophore and the gold surface. Although the oligoether chain is rather flexible, the positive charge on the Re(I) complexes and the positive charge on the DMAP molecules on the GNPs would experience electrostatic repulsion, preventing them from close contact to the GNP surface. For **4**-GNPs, the emission intensity was found to increase by about 2.5-fold (Figure 6b). Complex **5** has one $-(CH_2CH_2O)$ unit more than complex **4**, and the emission intensity of **5**-GNPs was found to increase by only about 1.4-fold (Figure 6c), in line with the increasing length of the oligoether spacer. Figure 6d showed the Stern−Volmer plots of the Re(I) complexes functionalized GNPs. The Stern−Volmer plot of **2**-GNPs was found to show a more upward deviation than that of **3**-GNPs, while the plot of **5**-GNPs showed an upward deviation that occurs to a smaller extent than **4**-GNPs. Such strong dependence of quenching efficiency on the length of the spacer was supportive of a dynamic energy transfer quenching mechanism, probably via the FRET mechanism.

## CONCLUSIONS

Transition metal complexes of ruthenium(II) and rhenium(I) have successfully been functionalized onto the surface of


dx.doi.org/10.1021/am500350c | ACS Appl. Mater. Interfaces 2014, 6, 6644−6653

DMAP capped GNPs without aggregation. The modified gold nanoparticles have been characterized. The emission intensity of both ruthenium(II) and rhenium(I) complexes has been shown to increase by 2.5-fold and 4.5-fold respectively upon prolonged treatment with esterase due to the release of GNP quencher upon hydrolysis of the ester linkage. The Ru(II) complex exhibited less emission recovery than the Re(I) complex as a result of the poorer spectral overlap between the Ru(II) complex and the SPR of the GNPs than that of the Re(I) complex. By studying the transient absorption and time-resolved emission decay of the free complexes, their modified GNPs, as well as the corresponding GNPs after treatment with esterase, the quenching mechanism in **1**-GNPs has been suggested to consist of a combination of charge transfer and dynamic energy transfer pathways while dynamic energy transfer was found to be the predominant quenching pathway in the **2**-GNP system. The energy transfer efficiency of the Re(I) modified GNPs has been found to be strongly dependent on the distance between the donor and the acceptor. A Förster resonance energy transfer (FRET) mechanism has been proposed for the observed dynamic energy transfer. It was believed that the present work has demonstrated a "proof-of-principle" assay method for the detection of esterase based on the FRET quenching of GNP-functionalized Ru(II) and Re(I) complexes. More importantly, this work has provided guiding principles for the modulation of FRET behavior via esterase hydrolysis and for the future design of novel inorganic−organic hybrids for molecular recognition and functions.

## ■ ASSOCIATED CONTENT

### Supporting Information

Experimental procedures, physical measurements and instrumentation, DLS particle size distribution, and FTIR spectra of the functionalized GNPs. This material is available free of charge via the Internet at http://pubs.acs.org.

## ■ AUTHOR INFORMATION

### Corresponding Author

*E-mail: wwyam@hku.hk

### Notes

The authors declare no competing financial interest.

## ■ ACKNOWLEDGMENTS

V.W.-W.Y. acknowledges support from The University of Hong Kong under the URC Strategic Research Theme on New Materials. This work has been supported by the University Grants Committee Areas of Excellence Scheme (AoE/P-03/08) and the General Research Fund (GRF) grant from the Research Grants Council of Hong Kong Special Administrative Region, China (HKU 7051/13P). F.C.-M.L. acknowledges the receipt of a University Postgraduate Studentship and A.Y.-Y.T. and V.K.-M.A. the receipt of a University Postdoctoral Fellowship, both administered by The University of Hong Kong. We also thank the Electron Microscope Unit at The University of Hong Kong for their technical assistance for TEM and EDX measurements.

## ■ REFERENCES

(1) Balzani, V.; Bergamini, G. Photochemistry and Photophysics of Coordination Compounds: Overview and General Concepts. *Top. Curr. Chem.* **2007**, *280*, 1−36.

(2) Ishow, E.; Credi, A.; Balzani, V.; Spadola, F.; Mandolini, L. A Molecular-Level Plug/Socket System: Electronic Energy Transfer from a Binaphthyl Unit Incorporated into a Crown Ether to an Anthracenyl Unit Linked to an Ammonium Ion. *Chem.—Eur. J.* **1999**, *5*, 984−989.

(3) Valeur, B.; Pouget, J.; Bourson, J.; Kaschke, M.; Ernsting, N. P. Tuning of Photoinduced Energy Transfer in a Bichromophoric Coumarin Supermolecule by Cation Binding. *J. Phys. Chem.* **1992**, *96*, 6545−6549.

(4) Hoeben, F. J. M.; Shklyarevskiy, I. O.; Pouderoijen, M. J.; Engelkamp, H.; Schenning, A. P. H. J.; Christianen, P. C. M.; Maan, J. C. E.; Meijer, W. Direct Visualization of Efficient Energy Transfer in Single Oligo(*p*-phenylene vinylene) Vesicles. *Angew. Chem.* **2006**, *118*, 1254−1258.

(5) Oh, E.; Hong, M. Y.; Lee, D.; Nam, S. H.; Yoon, H. C.; Kim, H. S. Inhibition Assay of Biomolecules based on Fluorescence Resonance Energy Transfer (FRET) between Quantum Dots and Gold Nanoparticles. *J. Am. Chem. Soc.* **2005**, *127*, 3270−3271.

(6) Takakusa, H.; Kikuchi, K.; Urano, Y.; Sakamoto, S.; Yamaguchi, K.; Nagano, T. Design and Synthesis of an Enzyme-Cleavable Sensor Molecule for Phosphodiesterase Activity Based on Fluorescence Resonance Energy Transfer. *J. Am. Chem. Soc.* **2002**, *124*, 1653−1657.

(7) Miyawaki, A.; Llopis, J.; Heim, R.; McCaffery, J. M.; Adams, J. A.; Ikura, M.; Tsien, R. Y. Fluorescent Indicators for $Ca^{2+}$ Based on Green Fluorescent Proteins and Calmodulin. *Nature* **1997**, *388*, 882−887.

(8) Zlokarnik, G.; Negulescu, P. A.; Knapp, T. E.; Mere, L.; Burres, N.; Feng, N.; Whitney, L.; Roemer, K.; Tsien, R. Y. Quantitation of Transcription and Clonal Selection of Single Living Cells with *β*-Lactamase as Reporter. *Science* **1998**, *279*, 84−88.

(9) Mochizuki, N.; Yamashita, S.; Kurokawa, K.; Ohba, Y.; Nagai, T.; Miyawaki, A.; Matsuda, M. Spatio-temporal Images of Growth-Factor-Induced Activation of Ras and Rap1. *Nature* **2001**, *411*, 1065−1068.

(10) Hanaoka, K.; Kikuchi, K.; Kojima, H.; Urano, Y.; Nagano, T. Development of a Zinc Ion-Selective Luminescent Lanthanide Chemosensor for Biological Applications. *J. Am. Chem. Soc.* **2004**, *126*, 12470−12476.

(11) Noh, Y. Y.; Lee, C. L.; Kim, J. J. Energy Transfer and Device Performance in Phosphorescent Dye Doped Polymer Light Emitting Diodes. *J. Chem. Phys.* **2003**, *118*, 2853−2864.

(12) Hong, X.; Zhang, C.; Liu, X.; Qiu, S.; Lu, P.; Shen, F.; Zhang, J.; Ma, Y. Atomic and Electronic Structure of Pyridine on Ge(100). *J. Phys. Chem. B* **2004**, *108*, 15229−15232.

(13) Baldo, M. A.; Forrest, S. R. Transient Analysis of Organic Electrophosphorescence: I. Transient Analysis of Triplet Energy Transfer. *Phys. Rev. B* **2000**, *62*, 10958−10966.

(14) Cleave, V.; Yahioglu, G.; Le Barny, P.; Friend, R. H.; Tessler, N. Harvesting Singlet and Triplet Energy in Polymer LEDs. *Adv. Mater.* **1999**, *11*, 285−288.

(15) Belser, P.; DeCola, L.; Hartl, F.; Adamo, V.; Bozic, B.; Chriqui, Y.; Mahadevan Iyer, V.; Jukes, R. T. F.; Kühni, J.; Querol, M.; Roma, S.; Salluce, N. Photochromic Switches Incorporated in Bridging Ligands: A New Tool to Modulate Energy-Transfer Processes. *Adv. Funct. Mater.* **2006**, *16*, 195−208.

(16) Chung, C. Y.-S.; Yam, V. W.-W. Induced Self-assembly and Förster Resonance Energy Transfer Studies of Alkynylplatinum(II) Terpyridine Complex through Interaction with Water-Soluble Poly(phenylene ethynylene sulfonate) and the Proof-of-Principle Demonstration of This Two-Component Ensemble for Selective Label-Free Detection of Human Serum Albumin. *J. Am. Chem. Soc.* **2011**, *133*, 18775−18784.

(17) Li, M.-J.; Kwok, W.-M.; Lam, W. H.; Tao, C.-H.; Yam, V. W.-W.; Phillips, D. L. Synthesis of Coumarin-Appended Pyridyl Tricarbonylrhenium(I) 2,2′-Bipyridyl Complexes with Oligoether Spacer and Their Fluorescence Resonance Energy Transfer Studies. *Organometallics* **2009**, *28*, 1620−1630.

(18) Yam, V. W.-W.; Song, H.-O.; Chan, S. T.-W.; Zhu, N.; Tao, C.-H.; Wong, K. M.-C.; Wu, L.-X. Synthesis, Characterization, Ion-Binding Properties, and Fluorescence Resonance Energy Transfer Behavior of Rhenium(I) Complexes Containing a Coumarin-Appended 2,2′-Bipyridine. *J. Phys. Chem. C* **2009**, *113*, 11674−11682.

(19) Woodroofe, C. C.; Won, A. C.; Lippard, S. J. Esterase-Activated Two-Fluorophore System for Ratiometric Sensing of Biological Zinc(II). *Inorg. Chem.* **2005**, *44*, 3112−3120.
(20) Kainmüller, E. K.; Ollé, E. P.; Bannwarth, W. Synthesis of a New Pair of Fluorescence Resonance Energy Transfer Donor and Acceptor Dyes and its Use in a Protease Assay. *Chem. Commun.* **2005**, 5459−5461.
(21) Li, M.-J.; Wong, K. M.-C.; Yi, C.; Yam, V. W.-W. New Ruthenium(II) Complexes Functionalized with Coumarin Derivatives: Synthesis, Energy-Transfer-Based Sensing of Esterase, Cytotoxicity, and Imaging Studies. *Chem.—Eur. J.* **2012**, *18*, 8724−8730.
(22) Prasad, B. L. V.; Sorensen, C. M.; Klabunde, K. J. Gold Nanoparticle Superlattices. *Chem. Soc. Rev.* **2008**, *37*, 1871−1883.
(23) Rosi, N.; Mirkin, C. A. Nanostructures in Biodiagnostics. *Chem. Rev.* **2005**, *105*, 1547−1562.
(24) Shi, W.; Sahoo, Y.; Swihart, M. T.; Prasad, P. N. Gold Nanoshells on Polystyrene Cores for Control of Surface Plasmon Resonance. *Langmuir* **2005**, *21*, 1610−1617.
(25) Mayilo, S.; Kloster, M. A.; Wunderlich, M.; Lutich, A.; Klar, T. A.; Nichtl, A.; Kürzinger, K.; Stefani, F. D.; Feldmann, J. Long-Range Fluorescence Quenching by Gold Nanoparticles in a Sandwich Immunoassay for Cardiac Troponin T. *Nano Lett.* **2009**, *9*, 4558−4563.
(26) Ray, P. C.; Fortner, A.; Darbha, G. K. Gold Nanoparticle Based FRET Asssay for the Detection of DNA Cleavage. *J. Phys. Chem. B* **2006**, *110*, 20745−20748.
(27) Thomas, K. G.; Kamat, P. V. Chromophore-Functionalized Gold Nanoparticles. *Acc. Chem. Res.* **2003**, *36*, 888−898.
(28) Katz, E.; Willner, I. Integrated Nanoparticle−Biomolecule Hybrid Systems: Synthesis, Properties, and Applications. *Angew. Chem., Int. Ed.* **2004**, *43*, 6042−6108.
(29) You, C.-C.; Verma, A.; Rotello, V. M. Engineering the Nanoparticle−Biomacromolecule Interface. *Soft Matter* **2006**, *2*, 190−204.
(30) Massue, J.; Quinn, S. J.; Gunnlaugsson, T. Lanthanide Luminescent Displacement Assays: The Sensing of Phosphate Anions Using Eu(III)−Cyclen-Conjugated Gold Nanoparticles in Aqueous Solution. *J. Am. Chem. Soc.* **2008**, *130*, 6900−6901.
(31) Elmes, R. B. P.; Orange, K. N.; Cloonan, S. M.; Williams, D. C.; Gunnlaugsson, T. Luminescent Ruthenium(II) Polypyridyl Functionalized Gold Nanoparticles: Their DNA Binding Abilities and Application as Cellular Imaging Agents. *J. Am. Chem. Soc.* **2011**, *133*, 15862−15865.
(32) Davies, A.; Lewis, D. J.; Watson, S. P.; Thomas, S. G.; Pikramenou, Z. pH-Controlled Delivery of Luminescent Europium Coated Nanoparticles into Platelets. *Proc. National Acad. Sci. U. S. A.* **2012**, *109*, 1862−1867.
(33) Li, M.-J.; Nie, M.-J.; Wu, Z.-Z.; Liu, X.; Chen, G.-N. Colorimetric and Luminescent Bifunctional Ru(II) Complex-Modified Gold Nanoprobe for Sensing of DNA. *Biosens. Bioelectron.* **2011**, *29*, 109−114.
(34) de Silva, A. P.; Fox, D. B.; Huxley, A. J. M.; McClenaghan, N. D.; Roiron, J. Metal Complexes as Components of Luminescent Signalling Systems. *Coord. Chem. Rev.* **1999**, *186*, 297−306.
(35) Ipe, B. I.; Yoosaf, K.; Thomas, K. G. Functionalized Gold Nanoparticles as Phosphorescent Nanomaterials and Sensors. *J. Am. Chem. Soc.* **2006**, *128*, 1907−1913.
(36) Wilton-Ely, J. D. E. T. The Surface Functionalisation of Gold Nanoparticles with Metal Complexes. *Dalton Trans.* **2008**, *37*, 25−29.
(37) Kamat, P. V. Photophysical, Photochemical and Photocatalytic Aspects of Metal Nanoparticles. *J. Phys. Chem. B* **2002**, *106*, 7729−7744.
(38) Huang, T.; Murray, R. W. Functionalized Gold Nanoparticles as Phosphorescent Nanomaterials and Sensors. *Langmuir* **2002**, *18*, 7077−7081.
(39) Gu, T.; Whitesell, J. K.; Fox, M. A. Energy Transfer from a Surface-Bound Arene to the Gold Core in ω-Fluorenyl-Alkane-1-Thiolate Monolayer-Protected Gold Clusters. *Chem. Mater.* **2003**, *15*, 1358−1366.
(40) Dulkeith, E.; Morteani, A. C.; Niedereichholz, T.; Klar, T. A.; Feldmann, J.; Levi, S. A.; van Veggel, F. C. J. M.; Reinhoudt, D. N.; Möller, M.; Gittins, D. I. Fluorescence Quenching of Dye Molecules near Gold Nanoparticles: Radiative and Nonradiative Effects. *Phys. Rev. Lett.* **2002**, *89*, 203002-1−203002-4.
(41) Sullivan, B. P.; Salmon, D. J.; Meyer, T. J. Mixed Phosphine 2,2′-Bipyridine Complexes of Ruthenium. *Inorg. Chem.* **1978**, *17*, 3334−3341.
(42) Wrighton, M.; Morse, D. L. Nature of the Lowest Excited State in Tricarbonylchloro-1,10-phenanthrolinerhenium(I) and Related Complexes. *J. Am. Chem. Soc.* **1974**, *96*, 998−1003.
(43) Bock, C. R.; Meyer, T. J.; Whitten, D. G. Photochemistry of Transition Metal Complexes. Mechanism and Efficiency of Energy Conversion by Electron-Transfer Quenching. *J. Am. Chem. Soc.* **1975**, *97*, 2909−2911.
(44) Balzani, V.; Bergamini, G.; Marchioni, F.; Ceroni, P. Ru(II)−Bipyridine Complexes in Supramolecular Systems, Devices and Machines. *Coord. Chem. Rev.* **2006**, *250*, 1254−1266.
(45) Puntoriero, F.; Campagna, S.; Stadler, A.; Lehn, J.-M. Luminescence Properties and Redox Behavior of Ru(II) Molecular Racks. *Coord. Chem. Rev.* **2008**, *252*, 2480−2492.
(46) Li, M.-J.; Chen, Z.; Zhu, N.; Yam, V. W.-W.; Zu, Y. Electrochemiluminescence of Ruthenium(II) Complexes Functionalized with Crown Ether Pendants and Effects of Cation Binding. *Inorg. Chem.* **2008**, *47*, 1218−1223.
(47) Li, M.-J.; Chu, B. W.-K.; Yam, V. W.-W. Synthesis, Characterization, Spectroscopic, and Electrochemiluminescence Properties of a Solvatochromic Azacrown-Containing Cyanoruthenate(II): Potential Applications in Separation and Indirect Photometric Detection of Cations and Amino Acids in HPLC. *Chem.—Eur. J.* **2006**, *12*, 3528−3537.
(48) Li, M.-J.; Ko, C.-C.; Duan, G.-P.; Zhu, N.; Yam, V. W.-W. Functionalized Rhenium(I) Complexes with Crown Ether Pendants Derived from 1,10-Phenanthroline: Selective Sensing for Metal Ions. *Organometallics* **2007**, *26*, 6091−6098.
(49) Yam, V. W.-W.; Lau, V. C.-Y.; Wu, L.-X. Synthesis, Photophysical, Photochemical and Electrochemical Properties of Rhenium(I) Diimine Complexes with Photoisomerizable Pyridyl-azo, -ethenyl or -ethyl Ligand. *J. Chem. Soc., Dalton Trans.* **1998**, 1461−1468.
(50) Ko, C.-C.; Ng, C.-O.; Feng, H.; Chu, W.-K. Synthesis, Characterisation and Photophysical Studies of Leucotriarylmethanes-Containing Ligands and Their Rhenium(I) Tricarbonyl Diimine Complexes. *Dalton Trans.* **2010**, *39*, 6475−6482.
(51) Gittins, D. I.; Caruso, F. Spontaneous Phase Transfer of Nanoparticulate Metals from Organic to Aqueous Media. *Angew. Chem., Int. Ed.* **2001**, *40*, 3001−3004.
(52) Gandubert, V. J.; Lennox, R. B. Assessment of 4-(Dimethylamino)pyridine as a Capping Agent for Gold Nanoparticles. *Langmuir* **2005**, *21*, 6532−6539.
(53) Massue, J.; Quinn, S. J.; Gunnlaugsson, T. Lanthanide Luminescent Displacement Assays: The Sensing of Phosphate Anions Using Eu(III)−Cyclen-Conjugated Gold Nanoparticles in Aqueous Solution. *J. Am. Chem. Soc.* **2008**, *130*, 6900−6901.
(54) Maccarini, M.; Briganti, G.; Rucareanu, S.; Lui, X.-D.; Sinibaldi, R.; Sztucki, M.; Lennox, R. B. Characterization of Poly(ethylene oxide)-Capped Gold Nanoparticles in Water by Means of Transmission Electron Microscopy, Thermogravimetric Analysis, Mass Density, and Small Angle Scattering. *J. Phys. Chem. C* **2010**, *114*, 6937−6943.
(55) Hostetler, M. J.; Green, S. J.; Stokes, J. J.; Murray, R. W. Monolayers in Three Dimensions: Synthesis and Electrochemistry of ω-Functionalized Alkanethiolate-Stabilized Gold Cluster Compounds. *J. Am. Chem. Soc.* **1996**, *118*, 4212−4213.
(56) Templeton, A. C.; Hostetler, M. J.; Warmoth, E. K.; Chen, S.; Hartshorn, C. M.; Krishnamurthy, V. M.; Forbes, M. D. E.; Murray, R. W. Gateway Reactions to Diverse, Polyfunctional Monolayer-Protected Gold Clusters. *J. Am. Chem. Soc.* **1998**, *120*, 4845−4849.

(57) Liu, Q.; Peng, J.; Li, F. High-Efficiency Upconversion Luminescent Sensing and Bioimaging of Hg(II) by Chromophoric Ruthenium Complex-Assembled Nanophosphors. *ACS Nano* **2011**, *5*, 8040−8048.
(58) Hallett, A. J.; Christian, P.; Jones, J. E.; Pope, S. J. A. Luminescent, Water-Soluble Gold Nanoparticles Functionalised with $^3$MLCT Emitting Rhenium Complexes. *Chem. Commun.* **2009**, *45*, 4278−4280.
(59) Terrill, R. H.; Postlethwaite, T. A.; Chen, C.-H.; Poon, C.-D.; Terzis, A.; Chen, A.; Hutchison, J. E.; Clark, M. R.; Wignall, G.; Londono, J. D.; Superfine, R.; Falvo, M.; Johnson, C. S., Jr.; Samulski, E. T.; Murray, R. W. Monolayers in Three Dimensions: NMR, SAXS, Thermal, and Electron Hopping Studies of Alkanethiol Stabilized Gold Clusters. *J. Am. Chem. Soc.* **1995**, *117*, 12537−12548.
(60) Gu, T.; Whitesell, J. K.; Fox, M. A. Energy Transfer from a Surface-Bound Arene to the Gold Core in $\omega$-Fluorenyl-Alkane-1-Thiolate Monolayer-Protected Gold Clusters. *Chem. Mater.* **2003**, *15*, 1358−1366.
(61) Griffin, F.; Fitzmaurice, D. Preparation and Thermally Promoted Ripening of Water-Soluble Gold Nanoparticles Stabilized by Weakly Physisorbed Ligands. *Langmuir* **2007**, *23*, 10262−10271.
(62) Liu, X.; Atwater, M.; Wang, J.; Huo, Q. Extinction Coefficient of Gold Nanoparticles with Different Sizes and Different Capping Ligands. *Colloids Surf., B* **2007**, *58*, 3−7.
(63) The overlap integral ($J$) were determined according to the following equation: $J = \int f_d(\lambda)\varepsilon_A(\lambda)\lambda^4\, d\lambda$. For complex **1**, $J = 2.11 \times 10^{19}$ $M^{-1}$ $cm^{-1}$ $nm^4$. For complex **2**, $J = 5.3 \times 10^{19}$ $M^{-1}$ $cm^{-1}$ $nm^4$. See Tan, C.; Atas, E.; Müller, J. G.; Pinto, M. R.; Kleiman, V. D.; Schanze, K. S. Amplified Quenching of a Conjugated Polyelectrolyte by Cyanine Dyes. *J. Am. Chem. Soc.* **2004**, *126*, 13685−13694.
(64) Pramod, P.; Sudeep, P. K.; Thomas, K. G.; Kamat, P. V. Photochemistry of Ruthenium Trisbipyridine Functionalized on Gold Nanoparticles. *J. Phys. Chem. B* **2006**, *110*, 20737−20741.
(65) Lomoth, R.; Häupl, T.; Johansson, O.; Hammarström, L. Redox-Switchable Direction of Photoinduced Electron Transfer in an $Ru(bpy)_3^{2+}$−Viologen Dyad. *Chem.—Eur. J.* **2002**, *8*, 102−110.
(66) Jebb, M.; Sudeep, P. K.; Pramod, P.; Thomas, K. G.; Kamat, P. V. Ruthenium(II) Trisbipyridine Functionalized Gold Nanorods. Morphological Changes and Excited-State Interactions. *J. Phys. Chem. B* **2007**, *111*, 6839−6844.
(67) Templeton, A. C.; Pietron, J. J.; Murray, R. W.; Mulvaney, P. Solvent Refractive Index and Core Charge Influences on the Surface Plasmon Absorbance of Alkanethiolate Monolayer-Protected Gold Clusters. *J. Phys. Chem. B* **2000**, *104*, 564−570.
(68) Kalyanasundaram, K.; Grätzel, M.; Nazeeruddin, Md. K. Luminescence and Intramolecular Energy-Transfer Processes in Isomeric Cyano-Bridged Rhenium(I)−Rhenium(I) and Rhenium-(I)−Ruthenium(II)−Rhenium(I) Polypyridyl Complexes. *Inorg. Chem.* **1992**, *31*, 5243−5253.
(69) Rajkumar, M.; Bhuvaneswari, J.; Velayudham, M.; Rajkumar, E.; Rajagopal, S. Photoluminescence Electron-Transfer Quenching of Rhenium(I) Complexes with Organic Sulfides. *J. Fluoresc.* **2011**, *21*, 1729−1737.
(70) Pacioni, N. L.; González-Béjar, M.; Alarcón, E.; McGilvray, K. L.; Scaiano, J. C. Surface Plasmons Control the Dynamics of Excited Triplet States in the Presence of Gold Nanoparticles. *J. Am. Chem. Soc.* **2010**, *132*, 6298−6299.